Sequential estimation of hydraulic parameters in layered soil using limited data

Katsutoshi Seki[a,b,*], Philippe Ackerer[b], and François Lehmann[b]

[a]*Natural Science Laboratory, Toyo University, Tokyo, Japan.*
[b]*Laboratory of Hydrology and Geochemistry, University of Strasbourg, Strasbourg, France.*
*Corresponding author. E-mail address: seki_k@toyo.jp (K. Seki).

Abstract

Field-scale estimation of soil hydraulic parameters is important for describing water movement in vadose zones. The importance of soil water measurements has been acknowledged with increasing soil water measurements becoming available; thus, the estimation of hydraulic parameters from observed soil water would be quite useful for hydrological modeling. This study estimated the hydraulic parameters of Brooks-Corey and Mualem model using the monitored soil water changes at two depths together with the rainfall intensity at two soil plots in a tropical rain forest in Indonesia. A one-dimensional multi-scale parameterization method was used for the analysis, beginning with homogeneous parameterization and identifying the depth of discontinuity using refinement indicators, thus increasing the number of zones. A method for sequential parameterization was developed in each step of zoning. The measured and simulated volumetric water contents with the optimized parameters showed good agreement for one plot (standard error is 0.0419) with 2-zone parameterization, and the effects of the initial parameters derived from different pedo-transfer functions on the optimized hydraulic functions were small, confirming the robustness of this method. However, at another field site, agreement between measured and simulated water contents was not very good (standard error is 0.0854), because the effect of the soil water repellency might have influenced the results, and the effects of the initial parameters were large. The algorithm proposed in this study systematically determines the hydraulic parameter set that describes field-scale water flow.

Keywords: Hydraulic properties, Unsaturated zone, Inverse modeling, Refinement indicator, Brooks-Corey model, Mualem model

1. Introduction

Soil water is an essential variable for understanding hydrological processes in vadose (unsaturated) zones and is important for various agricultural management practices, i.e., irrigation control, especially in arid and semi-arid regions in which water is a precious resource. Soil water is also important for climate modeling and numerical weather prediction. Recently, the importance of soil water monitoring has increased because of the need for climate change research. The Global Climate Observing System (GCOS) specified soil water as one of the Essential Climate Variables (ECVs) required to implement a comprehensive observation system to support scientific research on climate change (GCOS, 2010). Soil water is estimated using different methods, including in situ methods, satellite data, and hydrological models. Each method exhibits pros and cons, and hence, the integration of different techniques may decrease the drawbacks of a single given method (Brocca et al., 2011). The most reliable source of data is in situ measurements, and consequently, the need for direct soil water data is increasing.

To model vadose zone hydrology, it is important to characterize the hydraulic parameters that describe water movement in the vadose zones, i.e., parameters in soil water retention function and unsaturated hydraulic conductivity functions. It would be useful to obtain a reliable estimate of soil hydraulic parameters from soil water measurements which are becoming more easily available due to this increasing demand. However, inverse estimation of soil hydraulic parameters from field observed soil water content is difficult. Vereecken et al. (2008) compiled a review on soil water measurement in vadose-zone hydrology. After reviewing the extensive literature on the estimation of hydraulic properties in laboratory column experiments, this group noted that only a limited number of studies use field-scale soil water data to

inversely estimate the soil hydraulic properties. The authors argued that field studies remain limited because inverse estimation requires additional information, i.e., measured matric potential, soil structural information, homogeneous soil assumptions, measured values of hydraulic properties, well-defined flow conditions with gravity-dominated flow, and known bottom boundary conditions. With these restrictions, only a few field studies were used to estimate soil hydraulic parameters from soil water data under naturally occurring boundary conditions. Jacques et al. (2002) recorded the time series of water content, pressure head, and solute concentration under experimental field conditions and found that the observed data could be described by Richards' equation for water flow and the non-equilibrium convection-dispersion equation for solute transport with a layered soil profile. The authors were successful to inversely estimate the hydraulic parameters within the range of earlier determined parameters. Ritter et al. (2003) estimated hydraulic parameters from the measured time series of soil water content at three different depths, with the amount of irrigation measured by rain gauges and the reference evapo-transpiration estimated with weather data measured by an on-site weather station. The authors showed that inverse optimization is a promising parameter estimation procedure; however, it requires a well-posed inverse problem. In addition, considerable deviation was observed between the directly determined and inversely estimated soil water retention curves because soil water flow at the field scale is poorly represented by the soil retention curves directly measured at the core scale. Therefore, even if directly measured soil hydraulic parameters are available, it is better to obtain optimized hydraulic parameters from field observed data, which better represents the field scale water flow.

To optimize the hydraulic parameters of heterogeneous soil structure, Hayek et al. (2008) developed an algorithm for adaptive multi-scale parameterization. Usually, for optimization of heterogeneous soil hydraulic parameters, the structure of heterogeneity must be predetermined, and the depths of the discontinuity of the hydraulic parameters are specified. In the adaptive multi-scale parameterization method (Hayek et al., 2008), parameterization begins with the homogeneous soil structure, and detects the best depth for a new discontinuity by comparing the refinement indicator which shows the decrease of the objective function by increasing the number of zones, and the number of zones for parameterization increases stepwise. Hayek et al. (2008) conducted numerical experiments with noisy data and missing data and showed the efficiency and robustness of their algorithm. Sequential estimation of hydraulic parameters can stabilize the identification of parameters and avoid local minima of the objective function compared to a single-level strategy (Berre et al., 2009).

In this study, we estimated the soil hydraulic parameters of tropical forest soils from the monitored data on soil water contents and rainfall intensity. The soil water contents at two depths on 75 successive days with many rainfall events were used for the estimation. The one-dimensional multi-scale parameterization method developed by Hayek et al. (2008) was used for analysis of the heterogeneous soil structure to verify that it can be used with real field data. The objective of this study was to establish a method for estimating the soil hydraulic parameters that describe soil water behavior based on a limited field study dataset of soil water contents and rainfall.

2. Materials and Methods

2.1. Site Description and Soil Properties

Seki et al. (2010) measured soil hydraulic properties in a *Dipterocarpaceae* forest in Bukit Bangkirai on Borneo Island in Indonesia. Bukit Bangkirai is located close to the equator (1°1.5′S), and has a tropical rainforest climate with a high average annual temperature of 28°C and a heavy annual rainfall of 2500 mm. In this study, we focused on two plots, the K plot (K1 pit) and the HD plot with relatively flat soil surface, where continuous measurements were conducted.

In the K plot, root mats were observed in the 3-cm soil surface layer, below which lay a brown sandy clay loam layer. *Dipterocarpaceae* plants near the pit grew most of their root at the soil surface, where the root mats were observed. The clay content gradually increased to a depth of 60 cm. Based on the International Union of Soil Science classification, the soil texture was sandy clay loam to a depth of 40 cm, sandy clay within the 40 - 50 cm, and light clay within the 50 - 60 cm depths.

Two distinct soil layers were found in the HD plot: an upper quartz sand layer and a lower sandy loam layer. The upper sand layer was white in color and the lower sandy loam layer was brown in color, and therefore, the border between the two layers could be visually distinguished. The visible depth of the border fluctuated between 20 cm and 30 cm.

The soil water retention curves (SWRC) were measured by the hanging water column and pressure plate methods using two undisturbed samples of 5 cm diameter and 2.5 cm height from each plot sampled at the end of August 2006 (Fig. S1). The curves were fitted with the Brooks and Corey equation (Brooks and Corey, 1964) using SWRC fit software (Seki, 2007):

$$\begin{cases} S_e = \frac{\theta-\theta_r}{\theta_s-\theta_r} = (-\alpha h)^{-n} & \text{if } h < -1/\alpha \\ S_e = 1 & \text{if } h \geq -1/\alpha \end{cases} \quad (1)$$

where h is the soil water pressure head [L], θ is the volumetric water content [L^3 / L^3], θ_s is the saturated water content [L^3 / L^3], θ_r is the residual water content [L^3 / L^3], S_e is the effective saturation (also known as the normalized water content) [L^3 / L^3], and α [L^{-1}] and n [-] are parameters that determine the shape of the water retention curve, where 1/α is the air entry value (AEV). All the fitted curves were in good agreement ($R^2 > 0.98$) with the measured curves.

The saturated hydraulic conductivity K_s [L / T] was measured by the falling-head and constant-head methods using undisturbed soil cores of 5 cm diameter and 5 cm height. Three replicates were measured for every 5 cm from 5 cm to 50 cm depth, producing highly variable results. In the K plot, the average value was 1.77 x 10^{-3} cm/s, ranging from 1.18x10^{-4} cm/s to 1.10x10^{-2} cm/s. In the HD plot, the average value was 1.31 x 10^{-2} cm/s in the sand layer (upper layer) and 9.65 x 10^{-4} cm/s in the sandy loam layer (lower layer).

The soil water content was monitored with frequency domain reflectometry probes (ECH_2O sensors EC-10, Decagon Devices Inc.) at two locations in the K plot (10 cm, 20 cm) and the HD plot (20 cm, 30 cm) both not very close to the tree trumps from the end of September 2005 to the end of August 2006. Amount of rainfall was also measured in the HD plot; however, the data are available only until 20 December 2005 due to a fault in rainfall gauge.

2.2. Numerical Simulation

2.2.1 Description of the Forward Problem

The one-dimensional vertical model in the unsaturated water flow equation is expressed as Richards' equation (Richards, 1931) as follows:

$$\frac{\partial \theta}{\partial t} - \frac{\partial}{\partial z}\left[K(h)\left(\frac{\partial h}{\partial z} - 1\right)\right] = 0 \qquad (2)$$

where K is the hydraulic conductivity [L / T], z is the soil depth (taken as positive downwards) [L], and t is the time [T]. Based on the initial and boundary conditions (as described later), Richards' equation was solved using the Galerkin finite element method with an implicit scheme for time discretization. The discretized Richards' equation was resolved with a Fortran code using the Newton linearization method associated with the primary variable switching method (Lehman and Ackerer, 1997; Hayek et al., 2008).

To solve Richards' equation, the water retention function θ(h) and the hydraulic conductivity function K(h) must be defined. We used the hydraulic model of the Brooks and Corey Mualem-type equation (BC model). The hydraulic conductivity function of the BC model is derived by substituting the water retention function of the BC model (Eq. 1) into Mualem's function (Mualem, 1976), which produces the following equation:

$$K = K_S S_e^{\frac{2}{n}+\lambda+2} \qquad (3)$$

where λ [-] is the pore-connectivity parameter, which was estimated by Mualem (1976) as an average value of approximately 0.5 for many soils. Many researchers use the van Genuchten – Mualem type equation (VG model) (van Genuchten, 1980) to describe hydraulic properties; however, in this study, the BC model was selected because it has a distinct AEV shape. In the VG model, the shape of K(h) near saturation is quite steep, especially in fine-textured porous media, and numerical simulations often do not easily converge. Therefore, in finely textured material, another type of equation (Vogel and Cislerova, 1988) is used that introduces AEV into the VG model to make it easier for the numerical simulations to converge. The BC model already contains a distinct AEV defined by simple equations and therefore does not encounter a convergence problem near saturation. Therefore, we used the BC model in this study.

2.2.2. Domain

A one-dimensional vertical domain of 100-cm length was defined (Fig. 1). The length of the domain was determined from preliminary simulations with different length; 50-cm length was too short with wetting front easily reaching the bottom, while using 100 cm, 150 cm and 200 cm did not give so much different result. The element size was 0.5 cm at a depth of 0–50 cm and 1 cm at a depth of 50–100 cm, which produced 151 nodes in total. The domain was divided into multiple zones in which each zone exhibits unique hydraulic parameters. Because we used the BC model, in the case of homogeneous soil properties, the hydraulic parameters may be expressed with a parameter vector of six elements, i.e., $\mathbf{p}=(K_s, \theta_s, \theta_r, \alpha, n, \lambda)$ from Eqs. (1) and (3). In the case of multiple zones, zones 1 to nz, the parameter vector contains m = 6nz elements, i.e., $\mathbf{p}=(K_{s1}, \theta_{s1}, \theta_{r1}, \alpha_1, n_1, \lambda_1, \ldots, K_{snz}, \theta_{snz}, \theta_{rnz}, \alpha_{nz}, n_{nz}, \lambda_{nz})=(p_1, p_2, \ldots, p_m)$.

The simulation time covered 75 days beginning from October 1, 2005. The time variable t [T] was defined as t=0 at midnight of October 1, 2005 in this study.

2.2.3 Initial and Boundary Conditions

Almost no rainfall was observed for 50 days before the start of soil water monitoring; therefore, the water content at the start of monitoring (t=0) was quite low. At the K plot, the water content at the start of monitoring was 0.1 to 0.15, and by extrapolating with the soil water retention curve based on the BC function, it corresponded to a pressure head of -10000 cm or less. Considering this highly dry initial condition, -10000

cm was set as the initial pressure head in the entire domain.

A Neuman-type boundary condition of time-variable flux was used at the top of the profile (Neuman et al., 1974), and a zero-gradient drainage boundary condition, which simulates a freely draining soil profile that is not affected by the ground water table, was used at the bottom of the profile:

$$-K(h)\left(\frac{\partial h}{\partial z}-1\right)=q(t) \quad \text{with z=0 cm} \tag{4}$$

$$\frac{\partial h}{\partial z}=0 \text{ with z=100 cm} \tag{5}$$

where q(t) is the prescribed flux [L / T]. During the period of rainfall, the net flux was set to measured precipitation every hour, and during the period without rainfall, the net flux was set as the negative of the maximum potential rate of evaporation, -3.7 mm/day, as long as the surface pressure head was larger than the minimum pressure head, h_A, which was set to $h_A = -10^5$ cm (Scharnagl et al., 2011). When the surface pressure head became lower than h_A ($h < h_A$ at z=0), the upper boundary condition was changed to a constant pressure head of $h=h_A$. The maximum potential rate of evaporation was estimated from the FAO-adopted Penman-Monteith equation (Penman, 1948; Monteith, 1981; FAO, 1990) using the following values referring to regional climate data: temperature = 28°C, maximum daily temperature = 32°C, minimum daily temperature = 24°C, relative humidity = 0.78, atmospheric pressure = 100 kPa, and wind speed at 2 m height = 4 m/s.

2.2.4 Inverse Optimization and Multi-Scale Parameterization

The parameter vector was estimated by minimizing an objective function O(**p**), which was defined by the sum of the quadratic differences between the model-predicted water content and measured water content using the inverse optimization technique of the Levenberg-Marquardt method (Marquardt, 1963). Standard error (SE) can be calculated by O(**p**) with:

$$SE=\sqrt{\frac{O(\mathbf{p})}{N-1}} \tag{6}$$

where N is the numbers of optimized water content. The uncertainties in parameters p_k, Δp_k, are calculated as (Press et al., 1992):

$$\Delta p_k=\sqrt{O(p)}\sqrt{c_{kk}} \tag{7}$$

where c_{kk} is the covariance of the parameters p_k.

Forward calculation was conducted for the period from 0 days to 75 days, and the parameters were optimized from 30 days to 75 days to minimize the effect of error associated with the initial condition. Because we did not measure the initial soil water profile, the initial condition was subject to much uncertainty, and the predicted water content was rather inaccurate during the initial period. After 30 days of simulation with several infiltration and evaporation events, the simulated water profile with optimized parameters was expected to be closer to the real value. Therefore, we omitted the first 30 days of measurements, which contained larger errors compared with those of later periods from the objective function. The start day of 30 days was determined from several preliminary runs with different start periods.

An adaptive multi-scale parameterization algorithm (Hayek et al., 2008) was employed, which increases the number of degrees of freedom in a step-by-step manner (Fig. 2). A refinement indicator was defined to determine the optimal location of discontinuity for the next step. The first step consists of estimating the optimal parameters and the objective function in the case of one-zone parameterization with one parameter (homogeneous soil), and the refinement indicator for splitting the domain into two zones, Z_1 and Z_2, is defined by:

$$I=\left|\sum_{i\in Z_1}\frac{\partial O(p^{1*})}{\partial p_i}\right|=\left|\sum_{i\in Z_2}\frac{\partial O(p^{1*})}{\partial p_i}\right| \tag{8}$$

where I is the refinement indicator, p^{1*} is a parameter optimized with one-zone parameterization, and p_i is the parameter at node i. The refinement indicator was extended to the case of multi-dimensional parameters with a parameter vector of $\mathbf{p}=(p_1, p_2, \ldots, p_m)$. The refinement indicator corresponding to the parameter p_k at location i, $I_{k,i}$, was calculated from Eq. (8) by making p_k the only variable parameter, and the domain was split into zones Z_1 and Z_2 at the *i*th node. The refinement indicator depends on the unit of the parameter; therefore, a dimensionless refinement indicator was defined by $\bar{I}_{k,i}=\frac{I_{k,i}}{\max_i I_{k,i}}$. The multi-dimensional refinement indicator Γ_i was defined by:

$$\Gamma_i=\sum_{k=1}^{m}\bar{I}_{k,i} \tag{9}$$

The dimensionless multi-dimensional indicator, DMI, was defined by $\bar{\Gamma}_i=\frac{\Gamma_i}{\max_i \Gamma_i}$. The multi-dimensional parameterization algorithm is described as follows.

1. Choose an initial parameterization (usually one zone for the entire domain, nz=1; nz is the number of zones) P_{nz}, and an initial vector of parameters $\mathbf{p}^0$.
2. Minimize the objective function O(**p**), and compute the optimal solution $\mathbf{p}^{1*}$.
3. Choose a set of discontinuities that determines the next step of parameterization.
4. Compute the gradients $\partial O/\partial p_{k,i}$

5. For all selected discontinuities, compute the DMI.
6. Select a subset of discontinuities that have larger DMI than a certain value τ which is a user-defined value. Hayek et al. (2008) used τ =0.95 and τ =0.80. We used τ =0.95 in this study.
7. For all selected discontinuities, minimize the objective function O(**p**) corresponding to the new parameterization with inverse optimization.
8. Select the best parameterization (corresponding to the smallest objective function) for the next parameterization P_{nz+1} together with the corresponding discontinuity.
9. Stop the calculation if the stopping criteria are met. Otherwise, increase nz by 1, and return to step 4. The stopping criteria can be a specified number of zones or a threshold value for the objective function or objective function gradients, for example, less than 5% decrease in objective function or increase in model selection criteria such as AIC (Akaike information criterion) (Akaike, 1974) or BIC (Bayesian information criterion) (Schwarz, 1976).

AIC and BIC (also called SBC; Schwarz and Bayesian criterion) for log-likelihood function are (Rajkai et al., 2004):

$$AIC = N\ ln\left(\frac{O(p)}{N}\right) + 2m \quad (10)$$

$$BIC = N\ ln\left(\frac{O(p)}{N}\right) + m\ ln\ N \quad (11)$$

where m is the number of parameters. When models are compared in AIC or BIC, the model which has a smaller value of the criterion is the better model. BIC places more emphasis on the number of parameters in a model than AIC.

In the first step, we performed parameter optimization assuming that the soil contains uniform hydraulic properties. In this step, different strategies were applied between the K and the HD plots. In the K plot, where the fluctuation range of water contents was similar (0.22–0.38) at both of the measured depths of 10 cm and 20 cm, the water content at both depths was used for parameter estimation. In the HD plot, where the fluctuation range of water content differed with depth (0.09–0.31 at 20 cm, 0.3–0.53 at 30 cm), we used two strategies. The first strategy was the same as that of the K plot. The second strategy used the water content at one depth, the upper sand layer (depth of 20 cm), to calculate the objective function for homogeneous parameterization, and subsequently applied two-zone parameterization with the initial parameters as the optimized parameters of the upper layer and the hydraulic parameters at the bottom layer.

The BC model contains six parameters. Among the six parameters, many authors treat λ as a constant value of 0.5 to avoid over-parameterization; however, in certain cases, λ is also treated as a variable. Puhlmann et al. (2009) determined the soil hydraulic parameters of forest soil in a multistep outflow experiment and found that the λ values ranged from -5 to 5 (prescribed upper and lower limits). In this study, we treated λ as a constant at each step of parameterization, and the other five parameters (K_s, θ_r, θ_s, α, n) were optimized with a fixed λ value. After that, all six parameters (K_s, θ_r, θ_s, α, n, λ) were optimized.

Because hydraulic parameters are correlated, it is difficult to identify all of the parameters by inverse optimization. To resolve this problem, the soil hydraulic parameters may be fixed to certain a priori defined values (Jacques et al., 2002; Ritter et al., 2003). However, Scharmagl et al. (2011) noted that this approach might result in inappropriate parameter estimation, especially if the parameters are fixed at non-optimal values. By conducting numerical simulations, we found that it is sometimes more efficient to increase the degree of freedom sequentially. For example, among the five parameters (K_s, θ_r, θ_s, α, n), we first optimized three parameters simultaneously (K_s, θ_r, n) and subsequently optimized five parameters simultaneously.

We developed a new method, SRP; sequential optimization in the order of refinement indicator of parameters at the depth of discontinuity. From the definition of the refinement indicators, the parameter with the higher indicator value contributed more significantly to the minimization of the objective function. Hence, the parameters were optimized sequentially in the order of the refinement indicators. For example, when the refinement indicators at a depth of the first discontinuity are in the order of $\theta_s > \theta_r > n > \alpha > K_s$, in the 2-zone optimization, the parameters are optimized in five steps; (1) optimize θ_s, (2) optimize (θ_s, θ_r), (3) optimize (θ_s, θ_r, n), (4) optimize (θ_s, θ_r, n, α), and (5) optimize (θ_s, θ_r, n, α, K_s).

2.2.5. Initial Hydraulic Parameters

We used different sets of initial parameters to investigate the effect of the initial parameters on the result of parameter estimation (Table S1). The first parameter set, IP1, was taken from measured soil water retention curves and the measured saturated hydraulic conductivities, and the value of λ was assumed to be 0.5. Other initial parameter sets, IP2–IP5, were estimated from pedo-transfer functions. The pedo-transfer function (PTF) estimates the soil hydraulic parameters from known soil properties, i.e., soil texture, bulk density, and organic contents. The IP2 was obtained from the PTF of Wösten et al. (1999), which was derived from HYPRES, the database of soil hydraulic properties of European soils that predicts the

hydraulic parameters of the van-Genuchten Mualem model (VG model) from clay and silt content, organic matter content, and bulk density. The IP3 was obtained from the PTF of Rosetta software with the H3 (SSCBD) model (Schaap et al., 2001), which predicts VG parameters from sand, silt, clay, and bulk density based on a soil hydraulic database mostly from North America and Europe. The Rosetta model gives the prediction of both K_s and K_0, where K_s is the actual saturated hydraulic conductivity and K_0 is the matching point of the K(h) curve to saturation, which may differ from K_s. We used K_0 as the value of the initial parameter of K_s. The IP4 was obtained with the PTF of Teepe et al. (2003), which predicts VG parameters (except K_s and λ) from sand, silt, clay content and bulk density and is based on the measured soil water retention curves of forest soils. The K_s value was estimated from the PTF of Cosby et al. (1984), and the λ value was assumed to be 0.5. The IP5 was obtained from the PTF of Puhlmann and von Wilpert (2012), which predicts the VG parameters from soil texture, organic matter content, and bulk density based on the measurements of Puhlmann et al. (2009). The hydraulic parameters of VG models in IP2 to IP5 estimated from the PTFs were converted to the parameters of the BC model using the method developed by Lenhard et al. (1989), which was recommended by Ma et al. (1999), who compared it with other conversion methods (van Genuchten, 1980; Morel-Seytoux et al., 1996).

The PTFs used to derive IP2–IP5 were primarily constructed by analyzing the soil properties in Europe and America. Because this study analyses Indonesian soil, the estimated parameters are not at all similar to the measured parameter set of IP1 (Table S1). The functions of $\theta(h)$ and $K(h)$ at h=500 cm were also quite different from each other. The objective of using these uncertain initial parameter sets (IP2–IP5) was to investigate the robustness of parameter optimization in this study because it is not always possible to obtain measured hydraulic parameter sets for use as initial values.

3. Results

3.1. Homogeneous Parameterization

The result of simulation of the IP1 initial condition is shown first, and the results with the initial parameters of IP2–IP5 are shown in Section 3.4. For each plot, the parameters were optimized in 12 different ways (Table 1). For example, in the K plot, when five parameters (K_s, θ_s, θ_r, α, n) were optimized simultaneously, an objective function O(**p**) of 124.36 was obtained (denoted as "None" in the table). When K_s was fixed as a constant and the other four parameters (θ_s, θ_r, α, n) were optimized, O(**p**)=123.86 was obtained (first fit), and the estimated parameters of the first fit were used for the initial parameters in the second fit to optimize the five parameters simultaneously. At the end of the second fit, all of the parameters were optimized, and different parameters were obtained.

In the K plot, the fixed (θ_s, α) pair produced the minimum objective function, followed by fixing (θ_r, α) and (K_s, α) and the α–only method. The uncertainties in parameters p_k, Δp_k, of the second fit in the K plot are shown in Table S2. The magnitude of the parameter uncertainties differed among the fixed parameters. The coefficients of variability of the optimized parameters of these 12 optimization methods were, in descending order, 1.086 for θ_r, 0.752 for K_s, 0.403 for α, 0.228 for n, and 0.025 for θ_s. However, the soil water retention curves and unsaturated hydraulic conductivity functions drawn from these parameters were similar (Fig. 3A, 3B). Correlations among the estimated parameters of the 12 strategies were analyzed, and correlations were found in the (n, θ_r) pair ($R > 0.9$) and the (K_s, θ_s) pair ($R > 0.8$) (Fig. 3C, 3D). As evident from Fig. 3D, correlation between n and θ_r produced high variance in θ_r (CV=1.086). The coefficients of variability in θ and K calculated from the 12 sets of hydraulic parameters are shown in Fig. 4A.

In the HD plot, the first strategy with optimization of both measured depths resulted in a large objective function. With five-parameter optimization, O(**p**)=1011 was obtained, and with six-parameter optimization, O(**p**)=1007 was obtained. In the six-parameter optimization, a value of λ was optimized at -2.54. Because the result of homogeneous optimization was not a reliable estimate, five parameters were optimized for the initial parameter set of the two-zone parameterization method.

In the second strategy, only the measured water content at the top layer (20 cm) was used for the parameter optimization, and the corresponding results are shown in Table 1. The difference in the objective functions among 12 methods is not significant. The soil water retention curves and unsaturated hydraulic conductivity functions drawn from these parameters were similar, especially for a water content between 0.1 and 0.25 (Fig. 5A, 5B), and the measured water content at 30–75 days during the experiment mostly fell within this range. Correlations between parameters were found in the (n, θ_r) and (K_s, θ_s) pairs ($R > 0.9$) and the (K_s, α) pair ($R > 0.8$) (Fig. 5C, 5D). The coefficients of variability (CV) in θ and K calculated from the 12 sets of hydraulic parameters are shown in Fig. 4B. The CV was small in the middle range of the pressure head, but the values increased under highly wet and highly dry conditions.

For the different optimization methods shown in Table 1, the parameter sets were chosen that gave the smallest objective function: the fixed (θ_s, α) pair for

the K plot and the fixed (θ_r, α) pair for the HD plot. The six-parameter optimization was performed for the selected parameters; however, the objective function did not decrease in either the K or the HD plot. Therefore, the results of five-parameter optimization with λ=0.5 were determined to be the final optimization result of the homogeneous soil profile (Table 2).

3.2 Two-Zone Parameterization

The dimensionless multi-dimensional indicators for detection of the first discontinuity for the K plot and for the first strategy of the HD plot were calculated as shown in Fig. 6. We selected the discontinuity from 5-cm intervals except for the observation points, at the depth where the DMI was greater than τ =0.95, i.e., a depth of 15.25 cm (between the nodes of 15 cm and 15.5 cm) for the K plot. The optimized parameters obtained from the homogeneous parameterization were used for the initial parameters for two-zone parameterization with a discontinuity at a 15.25-cm depth. We compared three methods of optimization. The first method optimized 10 parameters, except for λ, which is held constant, at the same time. The second method fixed θ_s and α first to optimize 6 parameters (K_s, θ_r, n for 2 zones) and subsequently optimizing 10 parameters, which corresponds to the best strategy in the homogeneous optimization of the K plot in Table 1. The third method is SRP method, i.e., optimized the parameters in the order of the dimensionless indicators obtained in the homogeneous parameterization at a discontinuity depth of 15.25 cm. As a result, the objective functions for the first, second, and third methods were 101.11, 104.53, and 94.60, respectively.

Because the objective function of the third method, SRP, was the smallest, the parameter set estimated using the third method was selected. Parameterization with 12 parameters (including λ) decreased the objective function from 94.604 to 94.597, and this value was determined to be the optimized parameter in the two-zone parameterization (Table 3).

For the first strategy in the HD plot, the first discontinuity was selected at a depth of 25.25 cm, where the DMI was larger than τ =0.95 (Fig. 6), between the two measured depths of 20 cm and 30 cm. The refinement indicators at a depth of 25.25 cm were, in descending order, 0.9992 for α, 0.9986 for θ_r, 0.9971 for n, 0.9947 for θ_s, and 0.8065 for K_s. Therefore, the parameters were sequentially optimized in this order. As a result, an objective function of 26.14 was obtained, which was smaller than the objective function obtained with optimizing the 10 parameters at the same time. After that, 12-parameter optimization was conducted, and the objective function decreased to 24.38.

For the second strategy in the HD plot, a discontinuity was selected from the same depth as the first strategy, at 25.25 cm. The initial parameters of the upper zone (sand layer) were set to the result of homogeneous optimization, and the initial parameters of the lower zone (sandy loam layer) were taken from Table S1. By optimizing the 10 parameters simultaneously, we obtained an objective function of 23.33. With the two-step optimization methods of fixing (K_s, α), (θ_s, α), and (θ_r, α) first, we obtained objective functions of 26.20, 22.78, and 28.05, respectively. The parameter set that produced the minimum objective function of 22.78 was optimized again with 12 parameters, including λ, and the objective function slightly decreased from 22.780 to 22.779. Because the second strategy resulted in a smaller objective function compared with that of the first strategy, the second strategy was selected for the final parameter set, as shown in Table 3.

Fig. 7 compares the change in the measured and simulated water content and shows that two-zone optimization was effective in simulating the overall behavior of the soil water change at the two depths. However, this method did not simulate a portion of the water change accurately. In particular, the change in water content at a depth of 20 cm in the K plot was not well simulated. The simulated change in water content in response to rainfall during the period of 50 days to 75 days was more remarkable compared with the measured change.

Fig. 8 compares the water retention curves obtained by two-zone parameterization with measured data. The discrepancy between the measured and estimated water retention curves of the sandy loam layer in the HD plot was remarkable. This difference might be due to the transient nature of the actual soil profile. In the simulated parameterization, we clearly separated the two zones at one discontinuity depth; however, in the field, a transient zone of sand and sandy loam layer was present in which the soil of the two layers was mixed at a depth between 20 cm and 30 cm. In that transient zone, the soil property gradually shifted from sand to sandy loam. Therefore, the water retention curve measured from the upper region of the sandy loam layer might have displayed the averaged properties of sand and sandy loam.

3.3 Three-Zone Parameterization

The DMI for the second discontinuity was calculated for both the K and HD plots (Fig. S2). From the criterion of τ =0.95, eight depths were selected in the K plot (every 5 cm on the interval 60.5–95.5 cm), and one depth was selected in the HD plot (35.25 cm). The parameters were optimized for each discontinuity. To avoid parameters with unrealistic water content values, we always held the θ_r and θ_s values constant in a zone without an observation point. SRP method was conducted, and the discontinuity was selected from the

lowest O(**p**) value. The results of the three-zone parameterization are shown in Table S3. In the HD plot, the objective function decreased only 0.13%, from 22.78 in the two-zone parameterization to 22.75 in the three-zone parameterization. The objective function gradient was small and we stopped the calculation of the HD plot and used the two-zone parameterization for the final parameter set for the HD plot. In the K plot, the objective function decreased from 94.60 in the two-zone parameterization to 83.59 in the three-zone parameterization. Because we restricted θ_r and θ_s as constants in the third zone, the soil water retention curves did not deviate much from those of the second zone (Fig. S3). The hydraulic conductivity in the third zone of the K plot was lower compared with that of the second zone. This difference might reflect the observed fact that clay accumulates in the lower horizon. A comparison of the saturated hydraulic conductivity estimated from the simulation with the measured values is shown in Fig. S4. In the HD plot, the saturated hydraulic conductivity changed at a depth of 30 cm, whereas in this study, discontinuity was detected at 25 cm because the location of the core sampling for K_s measurement was not exactly the same as the location of the water content measurement.

We found the third discontinuity in the K plot at a depth of 85.5 cm to 95.5 cm (DMI > 0.95) and continued the calculation for four-zone parameterization using the same algorithm. The objective function did not decrease from that of the three-zone parameterization (83.59), and therefore, the iterations were stopped.

Model selection criteria are shown in Table S4. If we use AIC as a stopping criteria, three-zone parameterization is selected as the best parameterization for both K and HD plots. If we use BIC as a stopping criteria, three-zone parameterization is selected for K plot and two-zone parameterization is selected for HD plot.

3.4. Effect of Initial Parameters

Homogeneous parameterization and two-zone parameterization were conducted with the initial parameters derived from the PTFs (IP2–IP5) shown in Table S1 using a similar calculation procedure as that of the initial parameters of IP1. At each stage of optimization of the homogeneous and two-zone soil profiles, several methods of fixed parameters were compared: (1) fitting five parameters; (2) fixing the (K_s, α), (θ_s, α), and (θ_r, α) pairs first; and (3) SRP method, sequential optimization in the order of refinement indicator (excluding the second strategy in the HD plot).

The objective functions from two-zone parameterization are summarized in Table 4. Optimization with the PTF-derived initial parameters (IP2–IP5) produced smaller objective functions compared with the objective function derived from the measured parameters (IP1) for the K plot. For the HD plot, the overall performance of the second strategy was better compared with the first strategy. The soil water retention curves were drawn with the optimized parameter sets of each initial parameter set (Fig. 9) in which the result of the second strategy was used for the HD plot. In the K plot, IP2–IP5 had much larger AEV because the initial values of α were smaller (Table S1). In the HD plot, the estimated retention curves were similar, except for the near saturated region of the lower zone. Comparison of the simulated change in water content (Fig. S5) also showed that the uncertainty in the HD plot was small, whereas the uncertainty in the K plot was larger. Although the initial parameters were quite different, similar results were obtained for the HD plot, demonstrating the robustness of the method developed in this paper.

4. Discussion

The simulated water contents were not close to the measured water contents at certain depths and time periods. Several reasons might exist for this discrepancy, including (1) non-uniform water flow due to water repellency, (2) absence of pressure head measurement, (3) inaccuracy of rainfall data, (4) inaccuracy of potential evaporation, (5) effect of root uptake, (6) effect of seal and crust formation, (7) effect of hysteresis in soil water retention, and (8) effect of the calibration of soil water sensors.

(1) Soil water repellency causes rain water to infiltrate into the soil as preferential flow paths (Dekker and Ritsema, 1994). Kajiura et al. (2012) showed that water repellency of soil is affected by two factors: soil organic matter and water content. Strong water repellency was observed in the soil from the HD plot and in the 20-cm surface soil of the K plot (Seki et al., 2010); therefore, preferential flow might have existed in the infiltration process. The measured water change in the period from 50 days to 75 days at a 20-cm depth in the K plot (Fig. 7B) might have involved the process of preferential flow, i.e., rainwater primarily infiltrated in the preferential flow paths, which did not pass through the buried soil water sensor. This phenomenon might explain why the soil was not fully saturated after the heavy rainfall of 15 cm on day 51. Subsequently, the soil gradually became saturated following many rainfall events. Preferential flow can be modeled by the two-dimensional simulation (Ritsema and Dekker, 2000) or one-dimensional double continuum approach (Kordilla et al., 2012); however, the one-dimensional simulation in this study did not simulate the process well.

(2) Pressure head was not measured in this study,

which left uncertainty in the soil hydraulic properties. If the pressure head is measured with the water content, the water retention curve is actually measured in situ, and the uncertainty of the estimation of the soil water retention curve will decline, whereas the precision of the simulation will increase.

(3) Rainfall intensity was measured in the HD plot. The K plot was located 1 km away from the HD plot; hence, the rainfall intensity at the K plot might have differed from that at the HD plot. For example, the rainfall event of 24 mm on day 57.5 caused an increase in the measured water content in the HD plot but did not cause a similar increase in the measured water content in the K plot. The actual rainfall at this time might have been less in the K plot compared with that of the HD plot.

(4) In this study, direct measurements of such climate data as temperature and humidity were not available; hence, a rough estimate was used for potential evaporation. The accuracy of the potential evaporation may be improved by directly measuring the climate data and by treating potential evaporation as time variable. Temperature also affects hydraulic conductivity. As the study area is close to equator, temperature variation is smaller than higher latitude region, and fluctuation of temperature is smaller in soil than the ambient air. At the 10 cm depth of K plot, the difference in the maximum and minimum temperatures within the observation period of 75 days was only 2.4°C.

(5) The effect of root uptake in the root-mat zone was omitted in this study, which might also affect soil water behavior; therefore, introducing parameters for the distribution of root water uptake might improve the estimates.

(6) The effect of seal and crust formation at soil surface was neglected in this study. As the soil surface was covered with root mat, the effect of decrease in hydraulic conductivity due to crust formation should have been minimal.

(7) Hysteresis of water retention was omitted in this study. We used only one set of soil hydraulic parameters for each soil layer. Estimates might be improved using different soil hydraulic parameter sets for the wetting and drying processes.

(8) In this study, the water contents were measured by frequency domain reflectometry probes. The measured dielectric permittivity of the soil is usually converted to water content with an internal calibration equation provided by the manufacturer. Seki et al. (2010) measured the calibration curves for each soil sample collected from the field and found that the calibration equation in each soil was different than the manufacturer's given equation. In this study, soil-specific calibration equations were used; hence, the error in the calibration of sensors was minimized. The manufacturer says that with soil-specific calibration, the relative precision is 1 to 2 %. A general calibration curve is often used because it is time-consuming to obtain soil specific calibration curves. Therefore, error arising from the calibration curve might exist. Cardenas-Lailhacar and Dukes (2010) discussed the precision of several soil water sensors under field conditions.

By obtaining information on the above factors from direct observation, we might be able to obtain more precise estimates of the hydraulic parameters. We could also attempt to obtain additional points of depth to observe the water content and pressure head and improve precision. If observation of the above factors is unavailable, we could introduce new parameters for the unknown factors and increase the number of parameters for estimation. However, we should be careful when increasing the number of parameters because it does not always result in better estimates of unknown parameters. One reason for this is that as the number of unknown parameters increases, a combination of possible correlations between parameters increases, and therefore, the uncertainty of the estimated parameters may also increase. Another reason is that according to the parsimony criterion, among all models that fit the data, those with fewer parameters have higher posterior probabilities (Malinverno, 2002). Therefore, by introducing new parameters (i.e., root uptake, hysteresis, etc.), the predictive power of the estimated parameters would decrease. For the same reason, the zones should not be over-split to retain as small a number of parameters as possible.

Correlation was found between the estimated hydraulic parameters, as shown in Figs. 3C, 3D, 5C and 5D. Therefore, rather than verifying the uncertainty of individual parameters, it is better to verify the uncertainty of soil hydraulic functions, namely, water content and hydraulic conductivity at a certain pressure head. Uncertainty may be estimated by running several simulations with different initial parameter values and by drawing estimated soil water retention curves, as shown in Fig. 9. With known uncertainty in the results, the hydraulic parameter set obtained with this method could serve as good reference data about which parameters best describe the soil water change under specified field conditions.

5. Conclusion

Soil hydraulic parameters can be estimated from measured soil water contents and rainfall intensity using the multi-scale parameterization method. With the optimized parameters, the measured and simulated water contents showed quite good agreement in our analysis. As the water data is becoming more and more easily available and demand for estimation of

hydraulic parameter is increasing, this method can be applied to the field where only limited data is available. The original algorithm of Hayek et al. (2008) was improved using refinement indicators for determining not only the depth of discontinuity but also the sequence of parameters to be optimized. The measured values should be used for the initial parameters if they are available, but because they are not always available, hydraulic parameters estimated from pedo-transfer functions also can be used for the initial parameters. One of our results showed the robustness of our algorithm in which similar hydraulic functions were obtained for multiple simulations with different initial parameters; measured parameters, and parameters derived from four types of pedo-transfer functions. However, at another field site, agreement between measured and simulated water contents was not good and the robustness of the initial parameters were large. Therefore, uncertainty evaluation of the estimated hydraulic functions is recommended when applying this method to other locations.

References

Akaike, H., 1974. A new look at the statistical model identification. IEEE Trans. Automat. Contr., 19 (6), 716-723.

Berre, I., Lien, M.,Mannseth, T., 2009. Multi-level parameter structure identification for two-phase porous-media flow problems using flexible representations. Adv. Water Resour. 32, 1777-1788.

Brocca, L., Hasenauer, S., Lacava, T., Melone, F., Moramarco, T., Wagner, W., Dorigo, W., Matgen, P., Martínez-Fernández, J., Llorens, P., Latron, J., Martin, C., Bittelli, M., 2011. Soil moisture estimation through ASCAT and AMSR-E sensors: An intercomparison and validation study across Europe. Remote Sensing Env., 115.

Brooks, R.H., Corey, A.T., 1964. Hydraulic properties of porous media. Hydrol. Paper 3. Colorado State Univ., Fort Collins, CO, USA.

Cardenas-Lailhacar, B. Dukes, M.D., 2010. Precision of soil moisture sensor irrigation controllers under field conditions. Agric. Water Manage., 97, 666-672.

Cosby, B.J., Homberger, G.M., Clapp, R.B., Ginn, T.R., 1984. A statistical exploration of the relationships of soil moisture characteristics to the physical properties of soils. Water Resour. Res., 20(6), 682-690.

Dekker, L.W., Ritsema, C.J., 1994. How water moves in a water repellent sandy soil: 1. Potential and actual water repellency. Water Resour. Res., 30(9), 2507-2517.

FAO (Food and Agriculture Organization of the United Nations). 1990. Expert consultation on revision of FAO methodologies for crop water requirements. ANNEX V, FAO Penman-Monteith Formula, Rome Italy.

GCOS. 2010. Implementation plan for the Global Observing System for climate in support of the UNFCC (2010 Update).World Meteorological Organization, Geneva, Switzerland.

Hayek, M., Lehmann, F., Ackerer, P., 2008. Adaptive multi-scale parameterization for one-dimensional flow in unsaturated porous media. Adv. Water Resour., 31 (1), 28-43.

Jacques, D., Simunek, J., Timmerman, A., Feyen, J., 2002. Calibration of Richards' and convection-dispersion equations to field-scale water flow and solute transport under rainfall conditions. J. Hydrol., 259, 15-31.

Kajiura, M., Tokida, T., Seki, K., 2012. Effects of moisture conditions on potential soil water repellency in a tropical forest regenerated after fire. Geoderma,181-182, 30-35.

Kordilla, J., Sauter, M., Reimann, T., Geyer, T., 2012. Simulation of saturated and unsaturated flow in karst systems at catchment scale using a double continuum approach. Hydrol. Earth Syst. Sci., 16, 3909-3923.

Lehmann, F., Ackerer, P., 1997. Determining soil hydraulic properties by inverse method in one-dimensional unsaturated flow. J. Environ. Qual., 26, 76-81.

Lenhard, R.J., Parker, J.C., Mishra, S., 1989. On the correspondence between Brooks-Corey and van Genuchten models. J. Irrig. Drain. Eng., 115, 744-751.

Ma, Q., Hook, J.E., Ahuja, L.R., 1999. Influence of three-parameter conversion methods between van Genuchten and Brooks-Corey functions on soil hydraulic properties and water-balance predictions. Water Resour. Res., 35, 2571-2578.

Malinverno, A. 2002. Parsimonious Bayesian Markov chain Monte Carlo inversion in a nonlinear geophysical problem. Geophys. J. Int., 151, 675-688.

Marquardt, D.W. 1963. An algorithm for least-square estimation of nonlinear parameters. J. Soc. Ind. Appl. Math., 11, 431-41.

Monteith, J.L. 1981. Evaporation and surface temperature. Quarterly J. Royal Meteo. Soc., 107, 1-27.

Morel-Seytoux, H.J., Philip, D.M., Nachabe, M., Touma, J., van Genuchten, M.T., Lenhard, R.J., 1996. Parameter equivalence for the Brooks-Corey and van Genuchten soil characteristics: Preserving the effective capillary drive. Water Resour. Res., 32(5), 1251-1258.

Mualem, Y., 1976. A new model for predicting the hydraulic conductivity of unsaturated porous media. Water Resour. Res., 12(3), 513-522.

Neuman, S.P., Feddes, R.A., Bresler, E., 1974. Finite element simulation of flow in saturated-unsaturated soils considering water uptake by plants. Third Annual Report, Project No.A10-SWC-77, Hydraulic Engineering Lab., Technion, Haifa, Israel.

Penman, H.L. 1948. Natural evaporation from open water, bare soil and grass. Proc. Roy. Soc. A-Math. Phy., 193(1032), 120-145.

Press, W.H., Teukolsky, S.A., Vetterling W.T., Flannery, B.P., 1992. Numerical Recipes in Fortran 77. Second Edition. Cambridge University Press, Cambridge.

Puhlmann, H., von Wilpert, K., Lukes, M., Dröge, W., 2009. Multistep outflow experiments to derive a soil hydraulic database for forest soils. Eur. J. Soil Sci., 60, 792-806.

Puhlmann, H., von Wilpert, K., 2012. Pedotransfer functions for water retention and unsaturated hydraulic conductivity of forest soils. J. Plant Nutr. Soil Sci., 175, 221-235.

Rajkai, K., Kabos, S., van Genuchten, M.T., 2004. Estimating the water retention curve from soil properties: comparison of linear, nonlinear and concomitant variable methods. Soil Till. Res., 79, 145-152.

Richards L.A. 1931. Capillary conduction of liquids through porous medium. J. Appl. Phys., 1, 318-333.

Ritsema, C.J., Dekker, L.W., 2000. Preferential flow in water repellent sandy soils: principles and modeling implications. J. Hydrol., 231-232, 308-319.

Ritter, A., Hupet, F., Munoz-Carpena, R., Lambot, S., Vanclooster, M., 2003. Using inverse methods for estimating soil hydraulic properties from field data as an alternative to direct methods. Agric. Water Manage., 59, 77-96.

Schaap, M.G., Leij, F.J., van Genuchten, M.T., 2001. Rosetta: a computer program for estimating soil hydraulic parameters with hierarchical pedotransfer functions. J. Hydrol., 251, 163-176.

Scharnagl, B., Vrugt, J.A., Vereecken, H., Herbst, H., 2011. Inverse modeling of in situ soil water dynamics: investigating the effect of different prior distributions of the soil hydraulic parameters. Hydrol. Earth Syst.Sci., 15, 3043-3059.

Schwarz, G., 1976. Estimating the dimension of a model. Ann. Stat. 6, 461–464.

Seki, K. 2007. SWRC fit - a nonlinear fitting program with a water retention curve for soils having unimodal and bimodal pore structure. Hydrol. Earth Syst. Sci., 4, 407-437.

Seki, K., Suzuki, K., Nishimura, T., Mizoguchi, M., Imoto, H., Miyazaki, T., 2010. Physical and chemical properties of soils in the fire-affected forest of East Kalimantan, Indonesia. J. Trop. For. Sci., 22(4), 414-424.

Teepe. R., Dilling, H., Beese, F., 2003. Estimating water retention curves of forest soils from soil texture and bulk density. J. Plant Nutr. Soil Sci. 166, 111-119.

van Genuchten, M. 1980. A closed-form equation for predicting the hydraulic conductivity of unsaturated soils. Soil Sci. Soc. Am. J., 44, 892-898.

Vereecken, H., Huisman, J. A., Bogena, H., Vanderborght, J., Vrugt, J.A., Hopmans, J.W., 2008. On the value of soil moisture measurements in vadose zone hydrology: A review. Water Resour. Res., 44, W00D06.

Vogel, T., Cislerova, M., 1988. On the reliability of unsaturated hydraulic conductivity calculated from the moisture retention curve. Transport Porous Med., 3, 1-15.

Wösten, J.H.M., Lilly, A., Nemes, A., Le Bas, C., 1999. Development and use of a database of hydraulic properties of European soils. Geoderma 90, 169-185.

Table 1. Objective function with homogeneous parameterization for each plot. 1st fit was conducted by fixing the listed parameters and fitting other parameters. 2nd fit was conducted with 5 parameters. Numbers in parenthesis are iteration counts in optimization.

	K plot				HD plot[a]			
Fixed parameters	1st fit		2nd fit		1st fit		2nd fit	
None	-		124.36	(26)	-		38.26	(28)
K_s	123.86	(21)	123.67	(87)	38.48	(47)	38.48	(11)
θ_s	124.83	(21)	123.63	(22)	38.12	(28)	38.12	(11)
θ_r	123.93	(30)	123.93	(13)	38.00	(23)	38.00	(11)
α	119.40	(23)	118.90	(16)	37.81	(22)	37.783	(16)
n	128.54	(31)	128.54	(14)	38.08	(34)	38.02	(35)
K_s, θ_s	141.03	(20)	123.72	(27)	58.29	(20)	38.33	(31)
K_s, θ_r	123.22	(28)	123.19	(21)	37.93	(45)	37.93	(11)
K_s, α	118.29	(27)	118.29	(11)	38.18	(220)	37.94	(25)
θ_s, α	113.54	(26)	**113.50**[b]	(17)	38.49	(23)	38.23	(17)
θ_r, α	117.83	(24)	117.49	(16)	37.78	(23)	**37.776**[b]	(15)
K_s, θ_s, α	139.11	(22)	123.52	(22)	45.75	(24)	38.65	(43)

[a]Second strategy of fitting only one depth.
[b]Minimum objective function.

Table 2. Optimized parameters of homogeneous parameterization.

	Parameter	K plot	HD plot[a]
Initial	θ_r	0.0000	0.0244
	θ_s	0.3760	0.3150
	α (cm^{-1})	0.2260	0.1159
	n	0.1154	0.4684
	K_s (cm / s)	0.001771	0.013040
	λ	0.5000	0.5000
	O(p)	392.17	505.08
	SE	0.1740	0.2792
Optimized	θ_r	0.0976 ± 0.0135	0.0243 ± 0.0056
	θ_s	0.3756 ± 0.0140	0.3757 ± 0.0112
	α (cm^{-1})	0.2294 ± 0.1116	0.1141 ± 0.0529
	n	0.1122 ± 0.0087	0.3677 ± 0.0181
	K_s (cm / s)	0.00939 ± 0.011601	0.005394 ± 0.001351
	λ	0.5000	0.5000
	O(p)	113.50	37.78
	SE	0.0936	0.0764

[a]Second strategy of fitting one depth.

Table 3. Optimized parameters of two-zone parameterization.

Zone	Parameter	K plot	HD plot
Zone 1	Depth (cm)	0 - 15.25	0 - 25.25
	θ_r	0.0982	0.0843
	θ_s	0.3533	0.2806
	α (cm^{-1})	0.2120	0.1291
	n	0.0970	0.5484
	K_s (cm / s)	0.01321	0.07812
	λ	0.5000	0.4868
Zone 2	Depth (cm)	15.25 - 100	25.25 - 100
	θ_r	0.1500[a]	0.0249
	θ_s	0.3428	0.5186
	α (cm^{-1})	0.3201	0.2553
	n	0.0929	0.1143
	K_s (cm / s)	0.009314	0.0003328
	λ	0.5082	0.5001
	O(p)	94.60	22.78
	SE	0.0854	0.0419

[a]Upper limit value

Table 4. Objective function optimized with 2-zone parameterization.

Plot	Strategy	Initial parameters[a]				
		IP1	IP2	IP3	IP4	IP5
K plot		94.6 (c, e) [b]	76.8 (c, e)	77.81 (b, e)	76.0 (c, e)	76.8 (c, a)
HD plot	1st	26.1 (a, a)	23.7 (a, e)	24.5 (a, e)	55.7 (a, a)	26.3 (a, e)
	2nd	22.8 (d, c)	24.1 (c, a)	24.9 (b, a)	23.1 (b, a)	23.5 (a, b)

[a]Parameters shown in Table S1
[b]Selected strategy with minimum objective function in homogeneous and 2-zone parameterizations; a: fit 5 parameters, b: fix (K_s, α) first, c: fix (θ_s, α) pair first, d: fix (θ_r, α) pair first, e: SRP method.

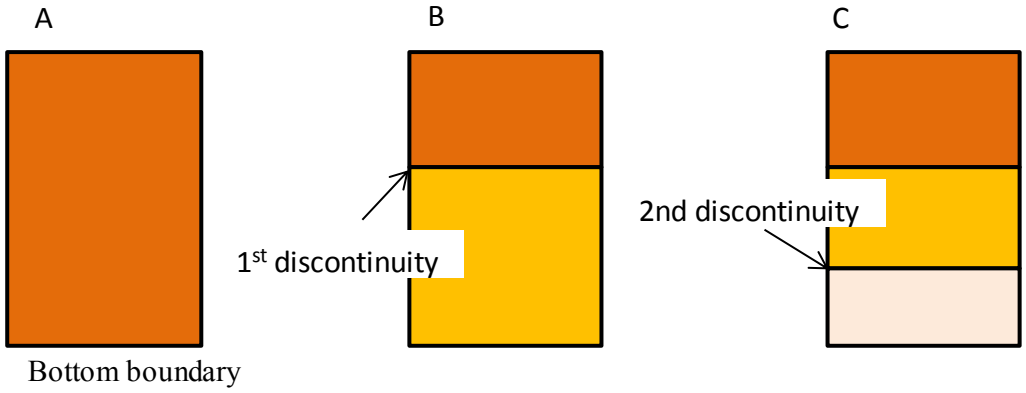

Fig. 1. Increasing heterogeneity step by step, (A) homogeneous parameterization, (B) 2-zone parameterization and (C) 3-zone parameterization with multi-scale parameterization method.

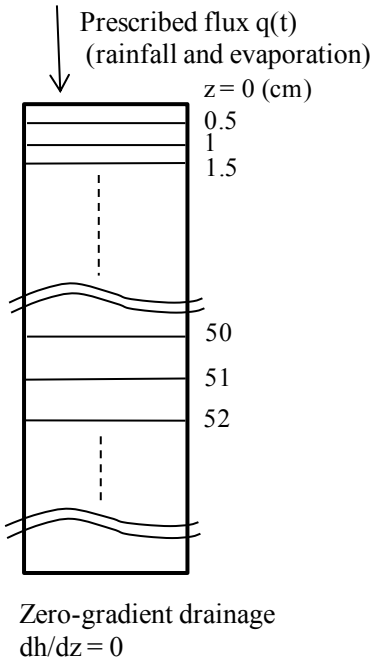

Fig. 2. Flow domain and boundary conditions.

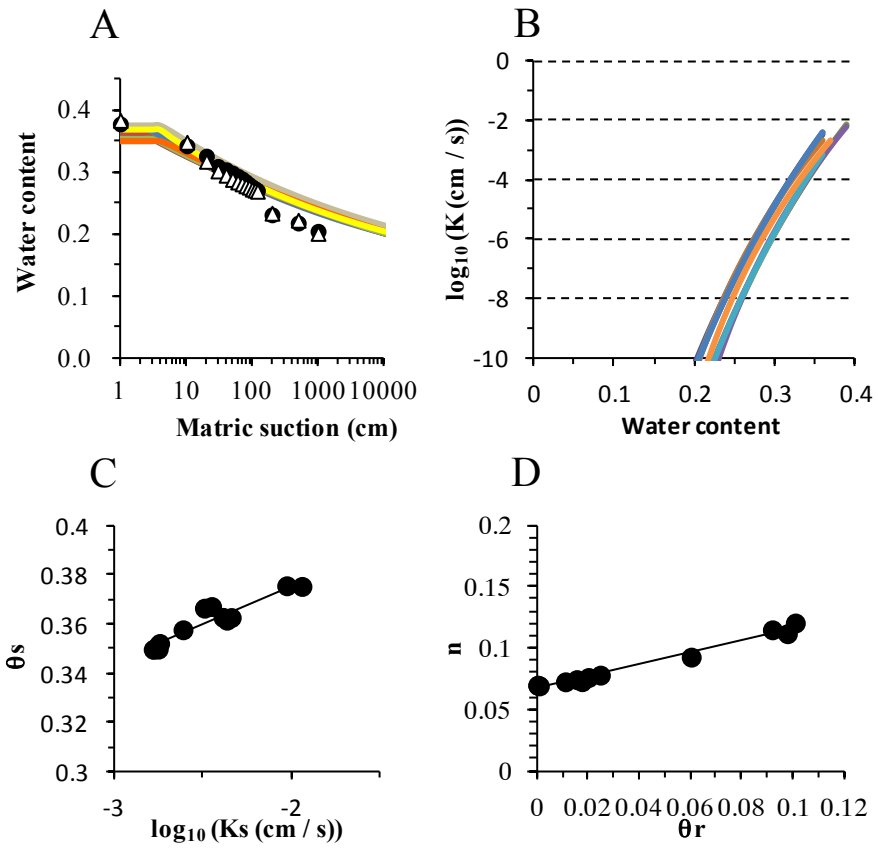

Fig. 3. Estimated hydraulic parameters with homogeneous parameterization in the K plot: (A) Soil water retention curves of 12 sets of estimated parameters (12 lines) and measured data (closed circle for 12.5–15 cm, open triangle for 20–22.5 cm); (B) K(θ) curves of 12 sets of estimated parameters; (C) Relationship between Ks and θs; (D) Relationship between θr and n.

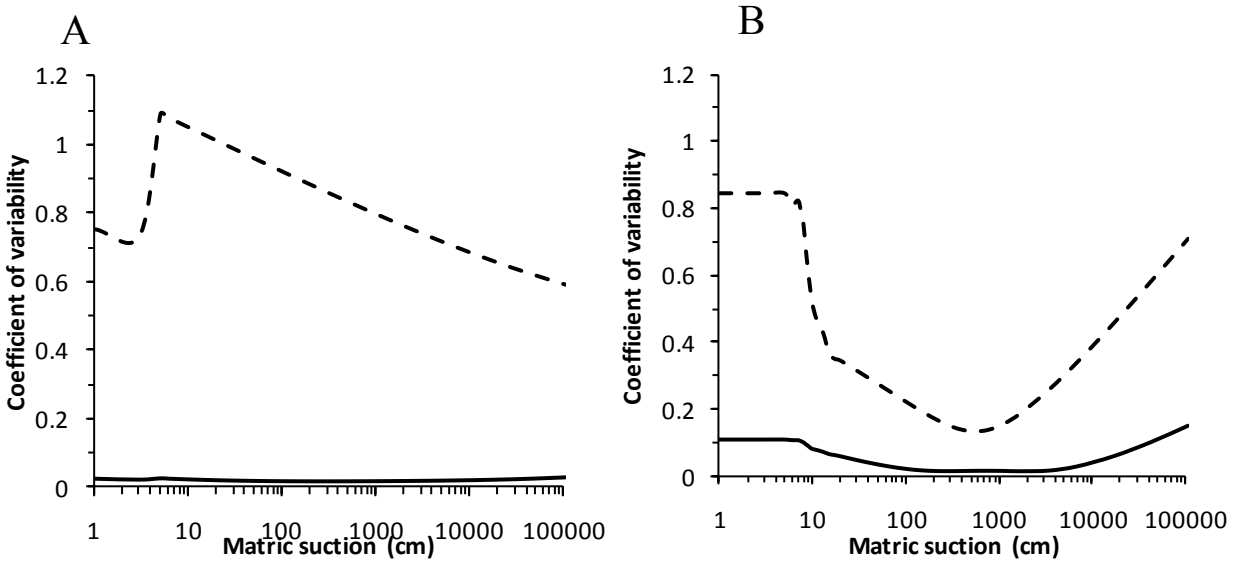

Fig. 4. Coefficient of variability (CV) of the water content and hydraulic conductivity in the estimated θ(h) (solid line) and K(h) (dotted line) functions with homogeneous parameterization in (A) the K plot and (B) the HD plot (second strategy).

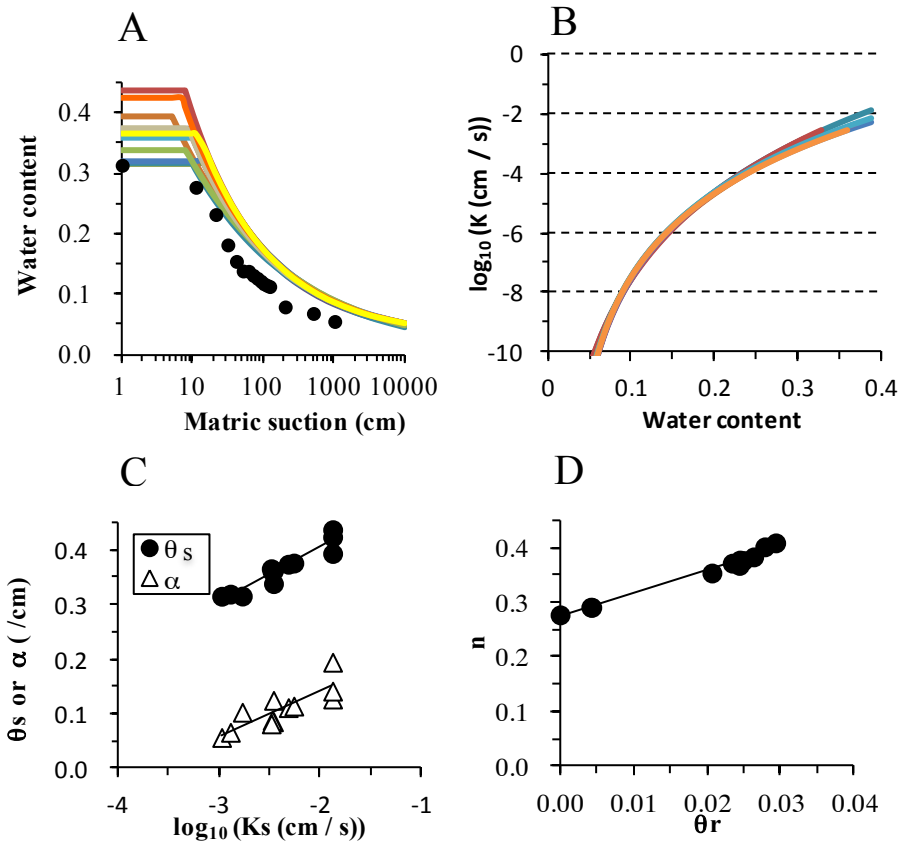

Fig. 5. Estimated hydraulic parameters of the sand layers with homogeneous parameterization (second strategy) in the HD plot: (A) Soil water retention curves of 12 sets of estimated parameters (12 lines) and measured data (closed circles); (B) K(θ) curves of 12 sets of estimated parameters; (C) Relationship between Ks and θs, a, respectively; (D) Relationship between θr and n.

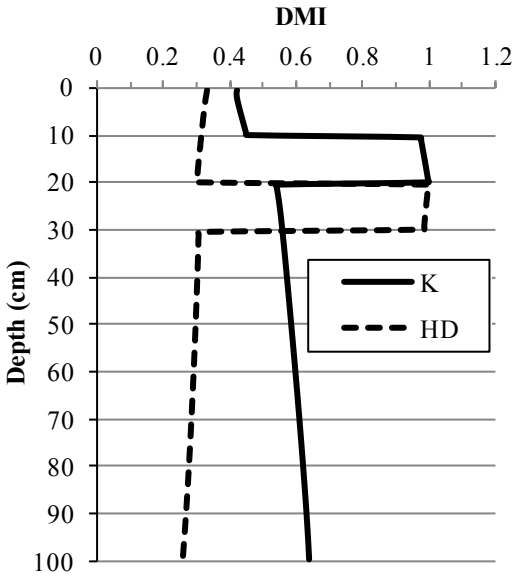

Fig. 6. Dimensionless multi-dimensional indicator (DMI) used to detect the first discontinuity of the K plot and the HD plot (first strategy).

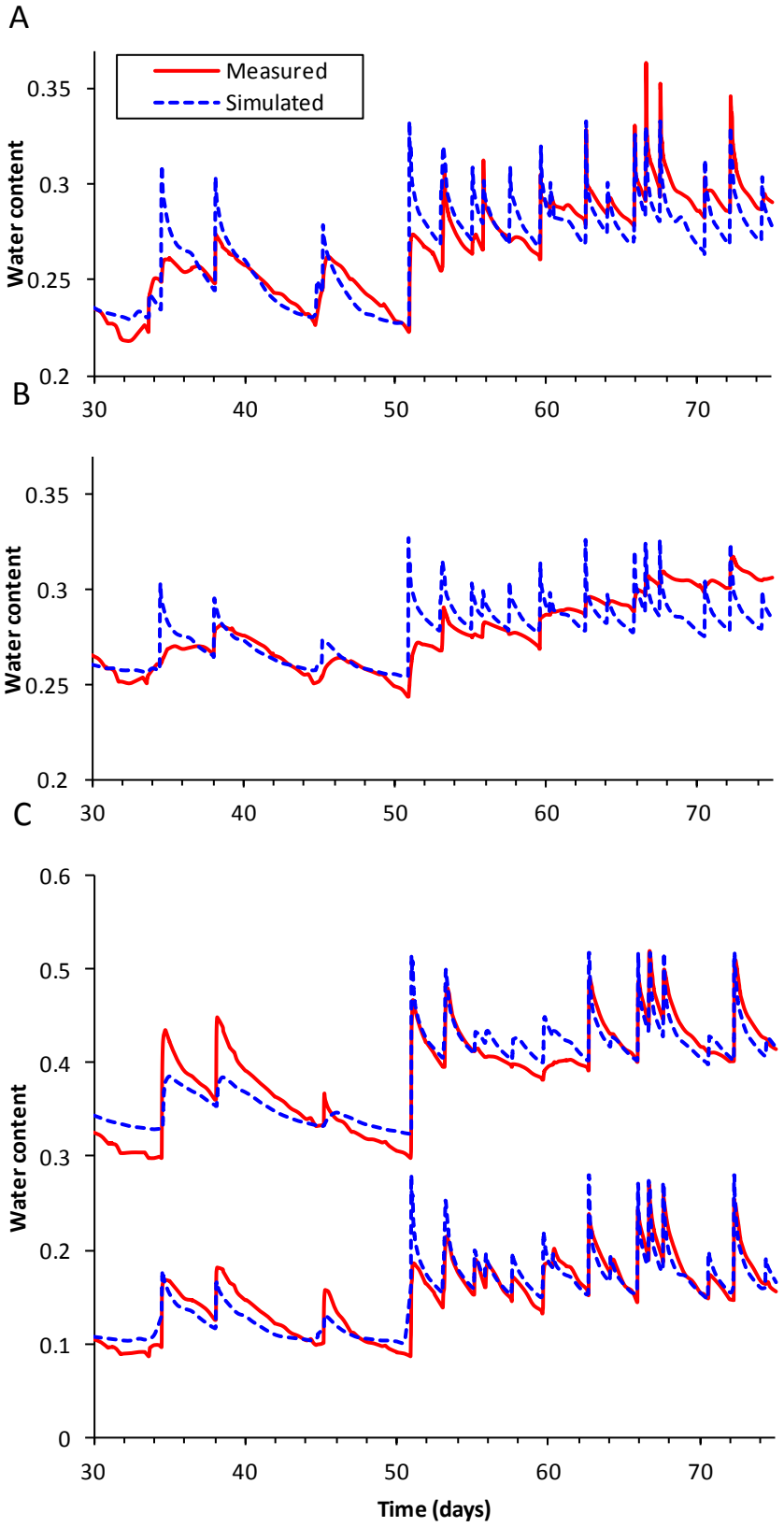

Fig. 7. Measured (solid red line) and simulated (dotted blue line) water content: (A) K plot, 10-cm depth; (B) K plot, 20-cm depth; (C) HD plot, 20-cm depth (sand layer, low water content) and 30-cm depth (sandy loam layer, high water content).

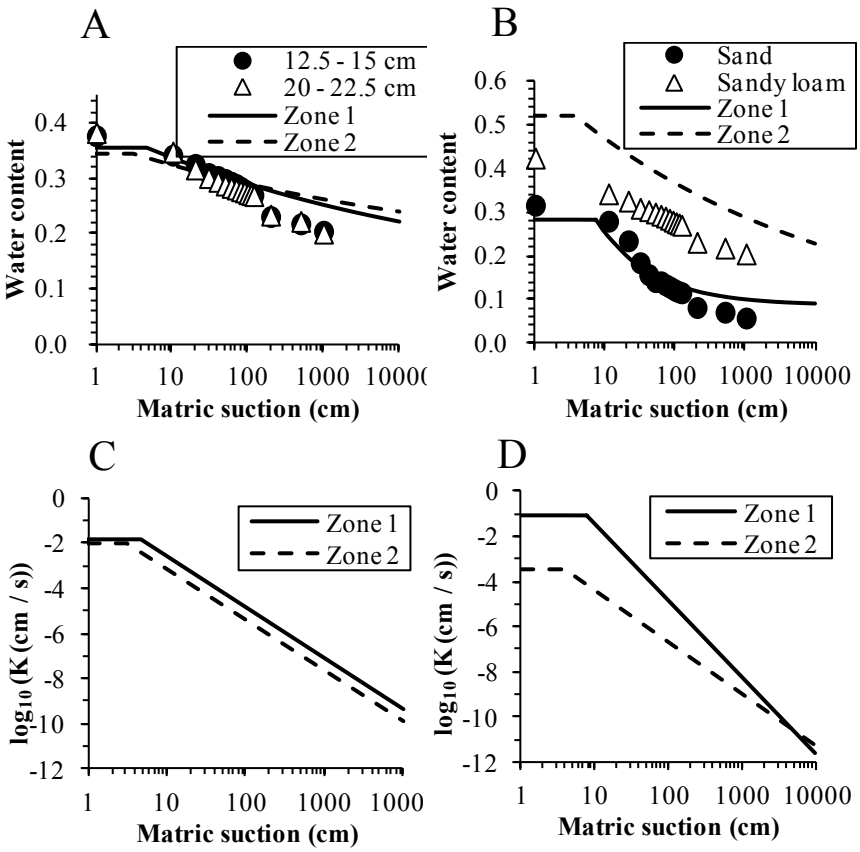

Fig. 8. Hydraulic functions of two-zone parameterization. Water retention function θ(h) of: (A) the K plot and (B) the HD plot with measured data (closed circles and open triangles, respectively) and the unsaturated hydraulic conductivity function K(h) of (C) the K plot and (D) the HD plot.

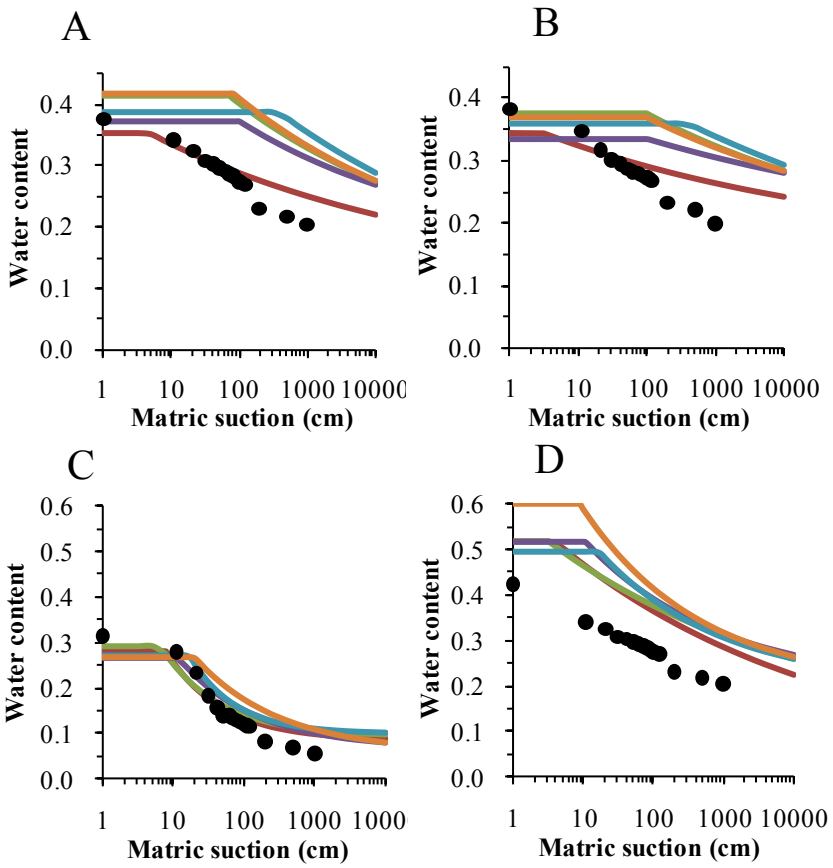

Fig. 9. Estimated soil water retention curves optimized with two-zone parameterization with different initial parameter sets: IP1 (red line), IP2 (green line), IP3 (purple line), IP4 (blue line), and IP5 (orange line). Closed circle represents measured data: (A) K plot, upper zone; (B) K plot, lower zone; (C) HD plot, upper zone; (D) HD plot, lower zone.

Supplementary data

Table S1. Initial hydraulic parameters of Brooks and Corey - Mualem model. IP1: Measured. 20-22.5 cm depth for K plot. IP2: PTF (pedotransfer function) of *Wösten et al.* (1999). IP3: PTF of Rosetta H3 model (*Schaap et al.*, 2001). IP4: PTF of *Teepe et al.* (2003) and *Cosby et al.* (1984). IP5: PTF of *Puhlmann and von Wilpert* (2012). PTF estimated van Genuchten parameters are converted to Brooks and Corey parameters.

Soil	Parameters	IP1	IP2	IP3	IP4	IP5
K plot	θ_r	0.0000	0.0100	0.0552	0.0000	0.0690
	θ_s	0.3760	0.3924	0.3771	0.4173	0.3901
	α (cm^{-1})	0.2260	0.0518	0.0223	0.0066	0.0256
	n	0.1154	0.1369	0.3839	0.1857	0.3462
	K_s (μm / s)	17.71	2.265	0.6510	4.997	1.774
	λ	0.5000	-3.7876	-0.7159	0.5000	-1.4980
	θ500	0.2179	0.2550	0.1829	0.3342	0.2018
	K500 (nm/s)	40.07	194.1	17.8	867.7	88.86
	O(p) [a]	392.17	1444.6	2772.1	1093.5	3614.8
HD plot	θ_r	0.0244	0.0100	0.0422	0.0000	0.0690
Sand	θ_s	0.3150	0.4309	0.4234	0.4833	0.4577
	α (cm^{-1})	0.1159	0.0877	0.0692	0.0103	0.0197
	n	0.4684	0.3515	0.7923	0.4587	1.0792
	K_s (μm / s)	130.40	6.3318	5.2782	39.52	11.5532
	λ	0.5000	-0.4782	-0.7928	0.5000	0.1068
	θ500	0.0678	0.1214	0.0652	0.2284	0.1019
	K500 (nm/s)	19.39	19.09	5.1	1183	6.446
	O(p) [a]	505.08	479.88	118.28	168.96	52.49
HD plot Sandy	θ_r	0.0000	0.0100	0.0561	0.0000	0.0690
Loam	θ_s	0.4230	0.5352	0.5244	0.6044	0.5001
	α (cm^{-1})	0.4620	0.0528	0.0399	0.0143	0.1123
	n	0.1170	0.1608	0.3695	0.2884	1.0505
	K_s (μm / s)	9.654	8.0458	2.8280	24.11	49.03
	λ	0.5000	-2.1185	-0.7478	0.5000	1.9021
	θ500	0.2238	0.3203	0.2110	0.3430	0.0753
	K500 (nm/s)	8.506	324.5	35.5	819.5	5.88.E-05
	O(p) [b]	509.30	96.38	65.43	426.11	1988.1

[a,b]Objective function with initial parameters with homogeneous soil profile (a) and 2-zone soil profile (b).

Table S2. Uncertainty of parameters of 2nd fit at K plot.

Fixed parameters	θ_r	θ_s	α (cm^{-1})	n	K_s (cm / s)
None	0.1951	0.3698	3.0668	0.1519	0.05938
K_s	0.0008	0.0020	0.0208	0.0006	0.00015
θ_s	0.0537	0.1045	1.9255	0.0341	0.04967
θ_r	0.0027	0.0070	0.1197	0.0018	0.00123
α	0.0081	0.0139	0.1078	0.0061	0.00216
n	0.0045	0.0072	0.1143	0.0045	0.00129
K_s, θ_s	0.1565	0.3201	2.8991	0.1103	0.05865
K_s, θ_r	0.0016	0.0045	0.0449	0.0011	0.00030
K_s, α	0.0019	0.0045	0.0285	0.0013	0.00042
θ_s, α	0.0135	0.0140	0.1116	0.0087	0.01160
θ_r, α	0.0072	0.0180	0.1153	0.0046	0.00144
K_s, θ_s, α	0.0620	0.0766	0.6236	0.0594	0.01370

Table S3. Optimized parameters of three-zone parameterization.

Zone	Parameter	K plot	HD plot
Zone 1	Depth (cm)	0 - 15.25	0 - 25.25
	θ_r	0.0982	0.0843
	θ_s	0.3533	0.2804
	α (cm^{-1})	0.2079	0.1291
	n	0.0969	0.5484
	K_s (cm / s)	0.02322	0.07812
	λ	0.5000	0.4868
Zone 2	Depth (cm)	15.25 - 60.5	25.25 - 35.25
	θ_r	0.1500[a]	0.0242
	θ_s	0.3428	0.5185
	α (cm^{-1})	0.3046	0.2553
	n	0.0926	0.1143
	K_s (cm / s)	0.03472	0.000333
	λ	0.5082	0.5001
Zone 3	Depth (cm)	60.5 - 100	35.25 - 100
	θ_r	0.1500[b]	0.0249[b]
	θ_s	0.3428[b]	0.5185[b]
	α (cm^{-1})	0.4073	0.2553
	n	0.0924	0.1143
	K_s (cm / s)	0.00620	0.000333
	λ	0.5082	0.5001
	O(p)	83.59	22.75
	SE	0.0803	0.0419

[a]Upper limit value
[b]Constant

Table S4. Statistical data and model selection criteria of each parameterization.

Plot	Zones	N	O(p)	SE	m	AIC	BIC
K plot	1	12960	113.5	0.09359	6	-61390	-61345
	2	12960	94.60	0.08544	12	-63739	-63649
	3	12960	83.59	0.08031	16	**-65334**[b]	**-65215**[b]
	4	12960	83.59	0.08031	20	-65326	-65177
HD plot[a]	1	6480	37.78	0.07636	6	-33326	-33285
	2	12960	22.78	0.04193	12	-82191	**-82101**[b]
	3	12960	22.75	0.04190	16	**-82200**[b]	-82080

[a]Second strategy of fitting only one depth.
[b]Minimum value of model selection criteria for each plot

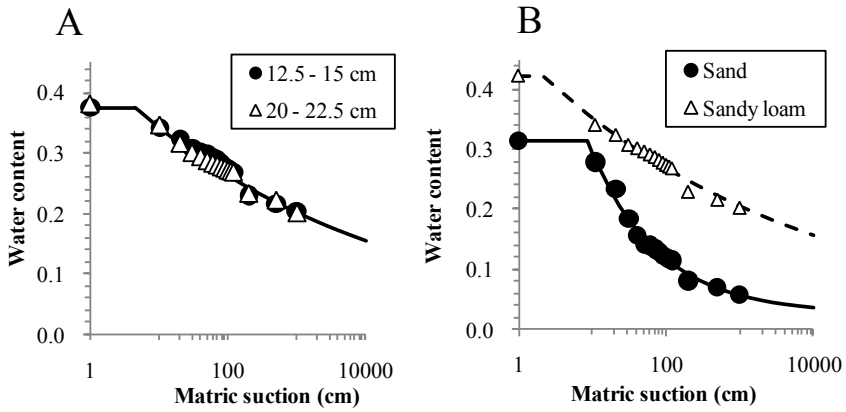

Fig. S1. Soil water retention curves of undisturbed soil samples. The measured curves are fitted with the Brooks and Corey equation. (A) Samples from 12.5-15 cm depth and 20-22.5 cm depth in the K plot. Only the curve fitted for 20–22.5 cm is shown. (B) Samples from 15-17.5 cm depth (sand layer) and 25-27.5 cm depth (sandy loam layer) in the HD plot.

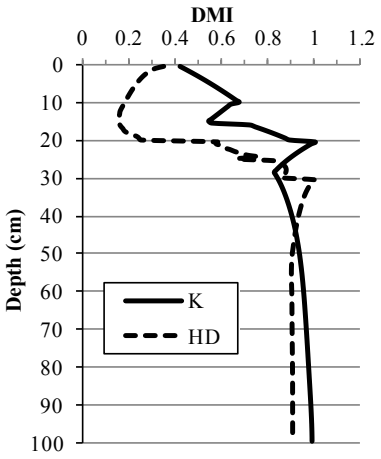

Fig. S2. Dimensionless multi-dimensional indicator used to detect the second discontinuity of the K plot and the HD plot.

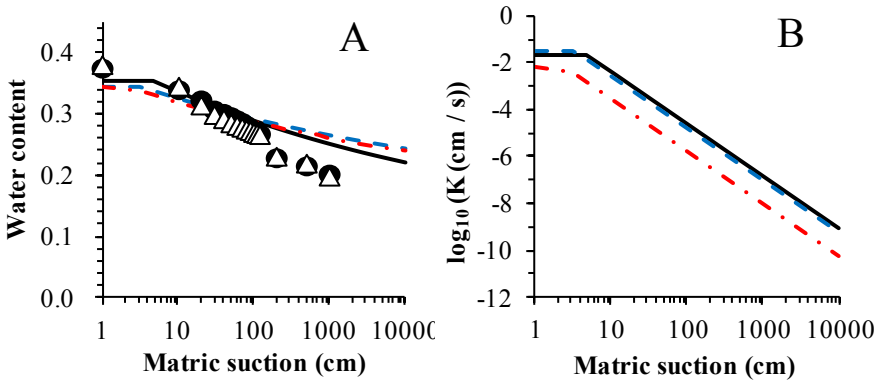

Fig. S3. Hydraulic functions of three-zone parameterization of the K plot. Solid black lines indicate zone 1, dashed blue lines indicate zone 2, and alternate long and short dashed lines in red indicate zone 3: (A) Water retention function q(h) with measured data (closed circle for 12.5–15 cm depth and open triangle for 20–22.5 cm depth); (B) Unsaturated hydraulic conductivity function K(h).

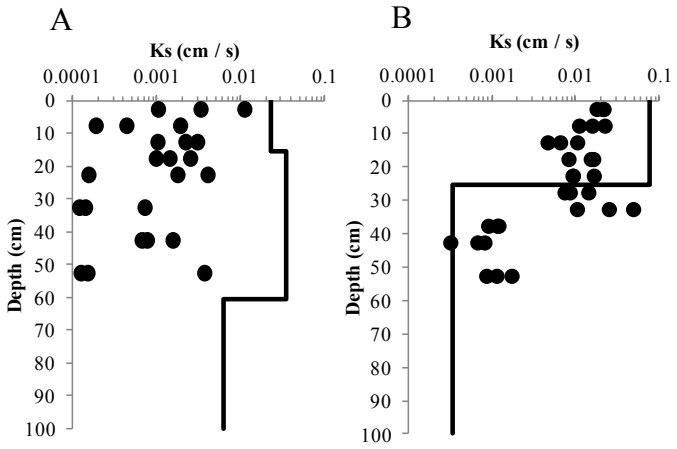

Fig. S4. Measured (closed circle) and simulated (solid line) saturated hydraulic conductivity: (A) K plot, 3-zone parameterization: (B) HD plot, 2-zone parameterization.

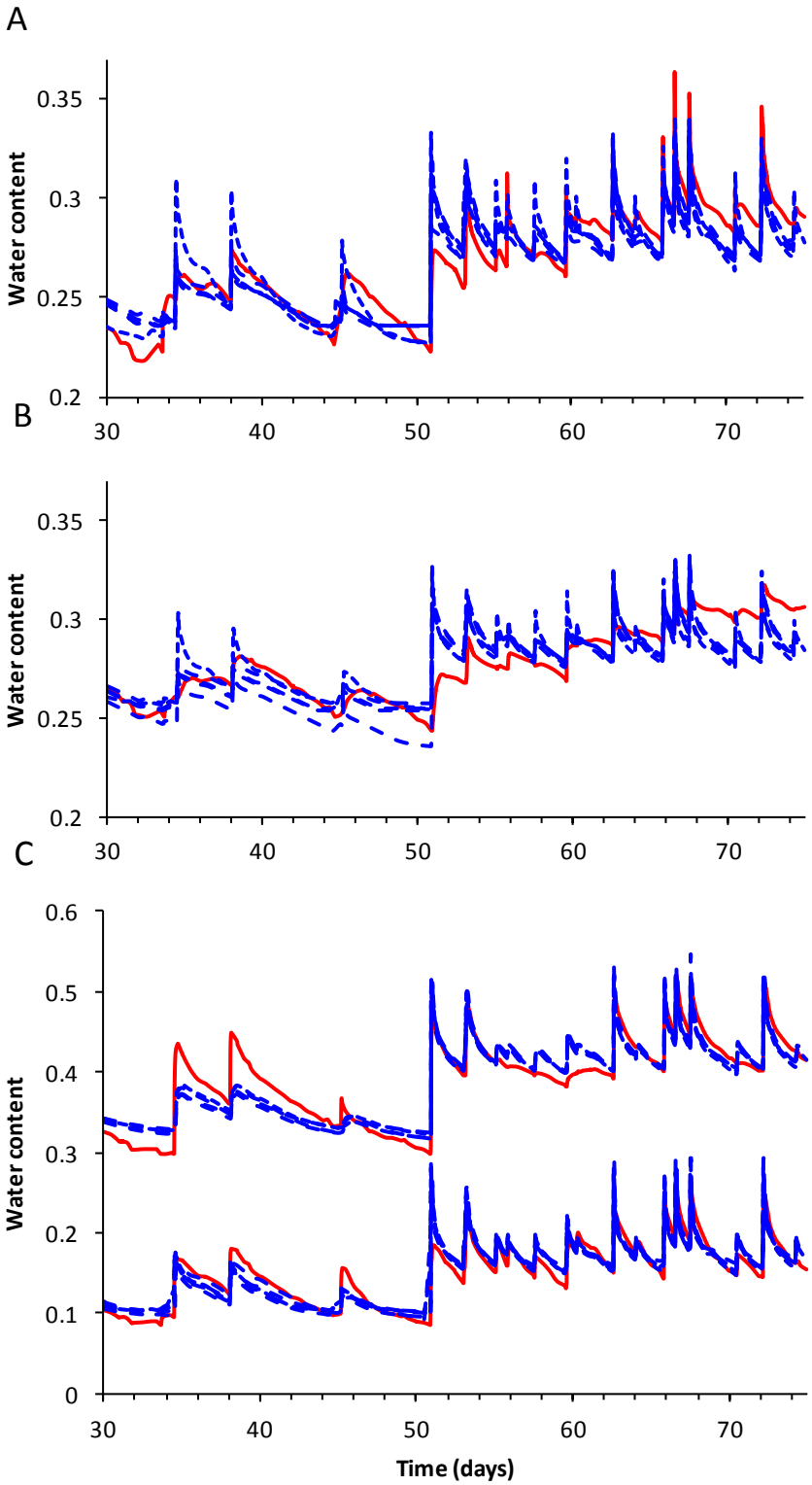

Fig. S5. Measured water content (solid red line) and simulated water content (dotted blue line) from five initial conditions: (A) K plot, 10-cm depth; (B) K plot, 20-cm depth; (C) HD plot, 20-cm depth (sand layer, low water content) and 30-cm depth (sandy loam layer, high water content).